

FACILE SYNTHESIS OF AgBr/ZnO NANOCOMPOSITE FOR ENHANCED PHOTODEGRADATION OF METHYLENE BLUE

L. ZHANG^{a*}, G. LIANG^b, Y. WU^c, Y. WAN^c

^aCollege of Medical Technology, Qiqihar Medical University, Qiqihar, Heilongjiang 161006, China.

^bCollege of Science, Qiqihar University, Qiqihar, Heilongjiang 161006, China.

^cCollege of Medical Technology, Qiqihar Medical University, Qiqihar, Heilongjiang 161006, China

In this paper, AgBr/ZnO nanocomposite was synthesized via a facile wet chemical method. The synthesized nanocomposite was characterized by SEM, XRD, UV-vis spectroscopy and photoluminescence spectroscopy. AgBr/ZnO nanocomposite displayed strong absorption in the visible light range. The prepared nanocomposite also exhibited a significant enhancement of photocatalytic activity towards degradation of methylene blue under visible light. The superior photocatalytic performance may be ascribed to the synergetic effects including visible light absorption extension, narrowed band gap and effective suppression of photogenerated electron-hole pairs.

(Received March 25, 2015; Accepted November 11, 2015)

Keyword: Nanocomposite, ZnO, AgBr, Photodegradation, Methylene blue

1. Introduction

In the past decade, semiconductors have attracted considerable attention because of their potential applications in solar cells, luminescent, electrical and optoelectronic devices and photodegradation of pollutants [1-3]. Among the semiconductors, ZnO is considered as one of the most potential candidates of photocatalyst due to its long-term stability, high photosensitivity and low price [4-6]. Recently, some report claimed that the ZnO has the better photocatalytic activity than TiO₂ [7]. However, like other metal oxide photocatalysts, the photocatalytic activity of ZnO is still restricted by fast recombination of the photogenerated electron hole pairs [8, 9]. Additionally, the ZnO only can absorb UV light with $\lambda < 387$ nm, which means only less than 5% of solar energy can be used for photocatalytic reaction. These drawbacks seriously restrict its application for industrial purposes. In order to overcome these drawbacks, a lot of approaches have been made for enhancing the photocatalytic activity of ZnO, such as metal ion doping [10, 11], non-metal doping [12], noble metal deposition [13, 14], coupling with other semiconductors [15], photosensitive material modification [16] and conjugated polymer modification [17, 18].

Silver halides are widely recognized as photosensitive materials [19-21]. It has been testified that the photocatalyst constituted by traditional semiconductor and silver halide has much higher photocatalytic activity than pure semiconductor [22-24]. For example, Hu et al. [25] reported the fabrication and characterization of and AgI/TiO₂ composite. The synthesized AgI/TiO₂ composite exhibited excellent photocatalytic activity for destruction of azo dyes under visible light illumination. Wang et al. [26] prepared mesoporous TiO₂ coated with Ag and AgBr nanoparticles. The prepared nanocomposite exhibited high photocatalytic activity for methyl orange degradation under visible light irradiation.

So far, many studies have been made for preparation of TiO₂-silver halide composite materials while only several studies reported the fabrication of ZnO-silver halide composite.

* Corresponding author: zhangliping36@yahoo.com

Herein, we report a facile chemical method for synthesizing AgBr/ZnO nanocomposite. The photocatalytic activities of the as-prepared AgBr/ZnO nanocomposite are investigated by photodegradation of methylene blue (MB) under the visible light illumination and the performance is compared with the bare ZnO.

2. Experimental

2.1 Materials

Zinc nitrate hexahydrate ($\text{Zn}(\text{NO}_3)_2 \cdot 6\text{H}_2\text{O}$), cetyltrimethylammonium bromide (CTAB), sodium borohydride (NaBH_4), silver nitrate (AgNO_3), methylene blue (MB), were purchased from Sigma-Aldrich. All other chemicals used were analytical grade reagents without further purification. Milli-Q water (18.2 M Ω cm) was used throughout the experiments.

2.2 Preparation of the AgBr/ZnO nanocomposite:

A typical procedure for the preparation of the AgBr/ZnO nanocomposite was as follows: As-received zinc nitrate hexahydrate (2 g) was dissolved in 10 mL of water under stirring. Then, 0.2 g CTAB was added into the solution for 10 min stirring. Afterward, 2 mL 20 mM AgNO_3 aqueous solution was added dropwise under continuous stirring. After addition of 1 mL NaBH_4 (0.5 M), the suspension was refluxed at 100°C for 3 h. The precipitate was collected by centrifugation followed with water wash. Pure ZnO sample was prepared using a similar method except addition of CTAB and AgNO_3 .

2.3 Photocatalytic degradation of MB

Photocatalytic activity of the samples was evaluated by photocatalytic degradation of MB aqueous solution under visible light irradiation. Typically, 30 mg of the prepared sample was added into 20 mL of MB solution (15 mg/mL) and kept under dark conditions for 30 min. After light illumination, 2 mL of suspension was then taken out a certain period and the photocatalyst was separated by centrifugation. The absorption of MB was then measured by a UV-vis spectroscopy. The absorbance of MB at 664 nm was used for measuring the concentration change

3. Results and discussion

SEM was used for observing the morphology of synthesized samples. Figure 1 shows the SEM images of pure ZnO and AgBr/ZnO nanocomposite. As can be seen, the pure ZnO formed using our wet chemical method showed a nanorod structure (Figure 1A). The length of ZnO nanorods is varying from 20-300 nm. However, the AgBr/ZnO nanocomposite formed in the same conditions showed a nanoflower structure with an average diameter of 132 nm. Moreover, the nanoflower shaped AgBr/ZnO nanocomposite exhibited a highly open morphologies than ZnO nanorod, which obviously produces more surface defects in tips and kink sites.[27, 28] During the photocatalysis, those surface defects can provide more active sites to photocatalyze dye molecules, thus accelerate the decomposition process.

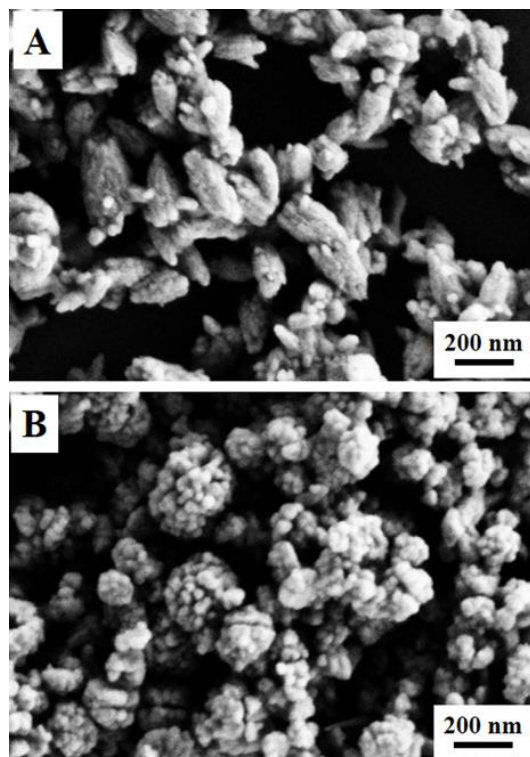


Fig. 1. SEM images of (A) ZnO and (B) AgBr/ZnO nanocomposite.

Fig. 2 demonstrates the XRD patterns of ZnO and AgBr/ZnO nanocomposite. The pure ZnO exhibits diffraction peaks at 32.1° , 34.3° , 36.2° , 47.3° , 56.2° , 62.7° , 67.0° , 68.1° and 69.5° can be indexed to hexagonal ZnO (JCPDS 36-1451). In XRD patterns of AgBr/ZnO, the peaks at 26.8° , 30.7° , 45.2° , 55.1° , 64.2° and 73.8° are corresponding to the cubic phase AgBr (JCPDS 06-0438). No additional peaks were observed corresponding to any other impurity phases, indicating the successful formation of nanocomposite with high purity.

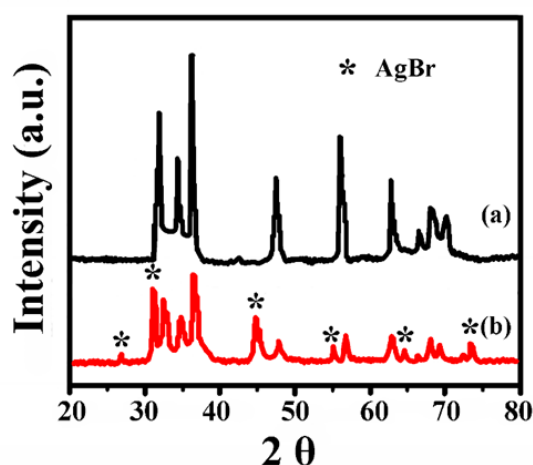


Fig. 2: XRD patterns of (a) ZnO and (b) AgBr/ZnO nanocomposite.

Fig. 3 shows the UV-vis diffuse reflectance spectra of the as-prepared ZnO and AgBr/ZnO nanocomposite. It can be seen that the spectrum of ZnO display a characteristic absorption peak around 300-400 nm. After incorporation with AgBr, the nanocomposite showed a less absorption intensity in the UV region. Also, AgBr/ZnO nanocomposite shows a relatively strong absorption at

visible region, indicating the AgBr/ZnO nanocomposite had optical capability in the whole range of visible light region spectrum [29]. Moreover, AgBr/ZnO nanocomposite also exhibits a broad peak at 500-700 nm, which could attribute to the red shift of absorption edge of AgBr [30, 31].

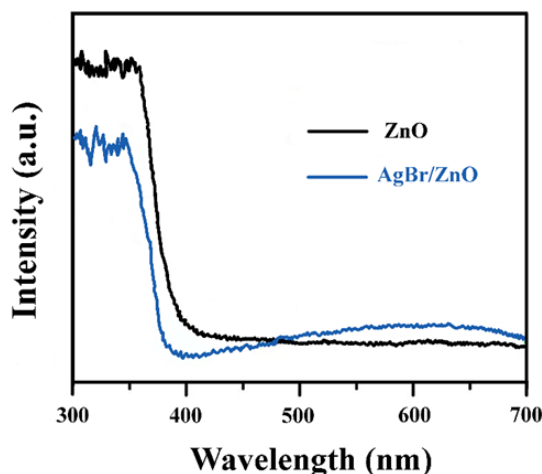


Fig. 3: UV-visible diffuse reflectance spectra of ZnO and AgBr/ZnO nanocomposite.

Fig. 4 shows the room temperature PL spectra of ZnO and AgBr/ZnO nanocomposite, which collected by the excitation wavelength of 325 nm. It can be observed that the spectrum of ZnO present a wide emission band in the wavelength range from 360 to 600 nm. The UV emission is attributed to the recombination of the photogenerated electron hole pairs [32]. The visible emission band is mainly ascribe to the recombination of electrons caused by structure defects such as zinc vacancies, oxygen vacancies and interstitial oxygen [33]. As can be seen, the AgBr/ZnO nanocomposite shows a similar emission band to those of pure ZnO and was in agreement with previously reports [34]. However, the emission of AgBr/ZnO spectrum shows a much weaker intensity compared with pure ZnO, indicating the suppression of the recombination of photogenerated electron-hole pairs [35].

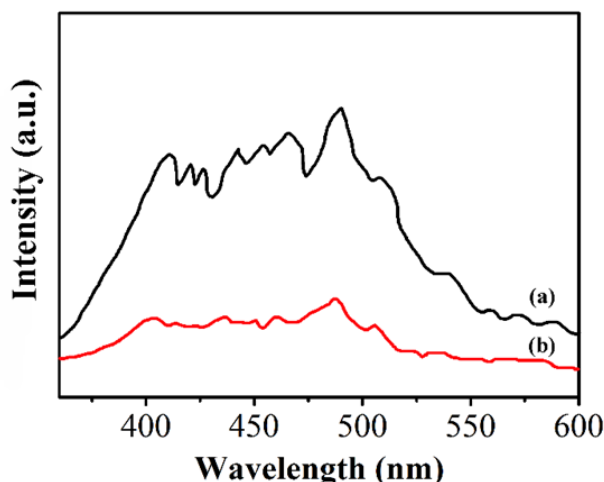


Fig. 4: Room temperature PL spectra of (a) ZnO and (b) AgBr/ZnO nanocomposite.

The photocurrent densities were performed on a CHI660A electrochemical workstation. The ZnO or AgBr/ZnO nanocomposite modified ITO worked as the photoanode, Pt wire as the counter electrode, and Ag/AgCl₃ as the reference electrode. 1 M H₂SO₄ was used as electrolyte. The photocurrent densities of ZnO and AgBr/ZnO nanocomposite were measured under visible illumination is shown in Figure 5. Results suggest that the both ZnO and AgBr/ZnO

nanocomposite show clearly current responses when the light is turned on and rapidly decrease the current to zero as soon as the light has been turned off. Also, the AgBr/ZnO nanocomposite shows a much higher photocurrent than that of ZnO, which further demonstrate that the AgBr/ZnO nanocomposite can effectively suppress photogenerated carriers recombination and probably could result in a higher photocatalytic performance.

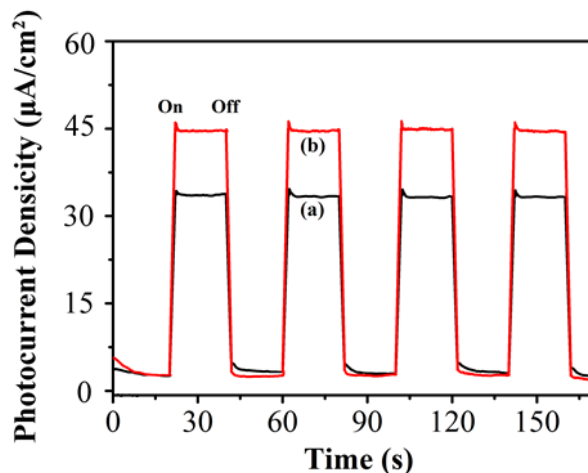


Fig. 5: Photocurrent densities vs. time for the (a) ZnO and (b) AgBr/ZnO nanocomposite under visible light illumination

The photocatalytic activity of synthesized AgBr/ZnO nanocomposite was evaluated by photodegradation of MB under visible light irradiation. Figure 6 shows the photodegradation profiles of C/C_0 using various photocatalysts. Where C_0 and C are the initial concentration of MB and concentration after irradiation, respectively. As shown in the figure, the MB shows a tiny self-degradation process after 180 min irradiation. The photodegradation rates of bare ZnO and P25 are 35% and 47% after 180 min irradiation, respectively. In contrast, the AgBr/ZnO nanocomposite exhibits a prominent performance, which can degrade more than 98% of MB in 180 min. The apparent rate constant of AgBr/ZnO nanocomposite (0.01664/min) was found to be almost 6-fold than that of ZnO (0.00266/min) and 4-fold than P25 (0.00353/min), which implies the introduction of AgBr could highly enhance the photodegradation rate.

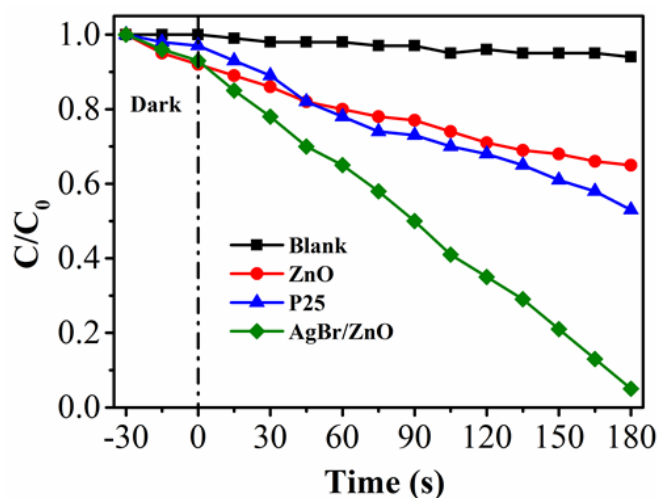


Fig. 6: Photodegradation profiles of MB using various photocatalyst under visible light illumination.

The stability of photocatalyst during photocatalytic reaction is a crucial consideration in the practical applications. Thus, the reusability test of the synthesized photocatalyst was carried

out using AgBr/ZnO nanocomposite for 4 photodegradation cycles. As shown in Figure 7, the AgBr/ZnO could remain more than 80% of photocatalytic performance after 4 cycles photodegradation, implying that the proposed nanocomposite has excellent stability. The slight decreasing performance might due to the photocatalysts loss during the washing process after each photodegradation cycle and surface retardant by organic intermediates.

On the basis of above mentioned performances, the probable mechanism of enhanced photocatalytic reaction is proposed as follow: The conduction band (CB) and valence band (VB) of ZnO are -4.3 and -7.5 eV, respectively. The CB and VB of AgBr are -3.7 and -5.95 eV, respectively. Therefore, the photogenerated electrons could be excited from VB to CB of AgBr, then transferred to ZnO [36]. The electrons transfer process is faster than the rate of electron hole recombination in AgBr, results in the separation of electron hole pairs, and enhances the photocatalytic performance of AgBr/ZnO.

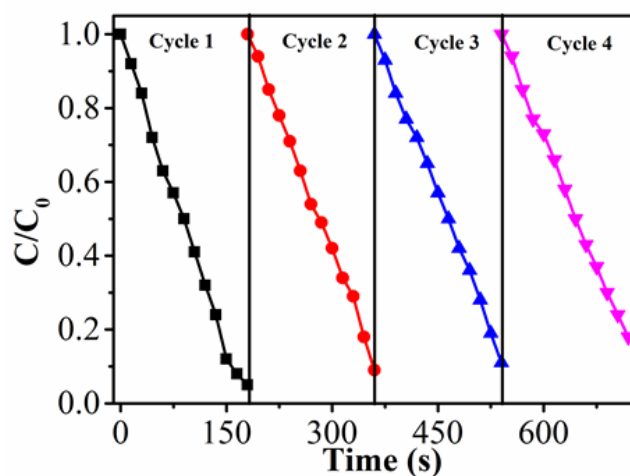


Fig. 7: Photocatalytic reusability test of AgBr/ZnO nanocomposite up to four cycles.

4. Conclusion

In summary, novel AgBr/ZnO nanocomposite was synthesized via a facile wet chemical method. AgBr/ZnO nanocomposite is found to be more efficient than bare ZnO commercial P25 for degradation of MB under visible light, which is mainly attributed to the stepwise energy level between ZnO and AgBr. Moreover, the reusability test showed that the AgBr/ZnO nanocomposite remained more than 80% photocatalytic activity in the fourth cycle, which made it highly promising for practical applications such as wastewater treatment.

Acknowledgments

This work was financially supported by the Scientific Research Foundation from Education Department of Heilongjiang Province (No. 12541910)

Reference

- [1] A. Suchodolskis, A. RĖza, V. Bukauskas, A. Mironas, A. Šėtkus, I. ŠimkienĖ, *Materials Science* **20**, (2014).
- [2] O. Zuas, N. Hamim, *Materials Science* **19**, (2013).
- [3] L. Fu, W. Cai, A. Wang, Y. Zheng, *Materials Letters* **142**, 201 (2015).
- [4] B. StypuŁa, A. Kmita, M. Hajos, *Materials Science* **20**, (2014).
- [5] L. Fu, Z. Fu, *Ceram Int* **41**, 2492 (2015).

- [6] L. Fu, T. Xia, Y. Zheng, J. Yang, A. Wang, Z. Wang, *Ceram Int* **41**, 5903 (2015).
- [7] S. Sakthivel, B. Neppolian, M.V. Shankar, B. Arabindoo, M. Palanichamy, V. Murugesan, *Solar Energy Materials and Solar Cells* **77**, 65 (2003).
- [8] Q. Wang, N. Plylahan, M.V. Shelke, R.R. Devarapalli, M. Li, P. Subramanian, T. Djenizian, R. Boukherroub, S. Szunerits, *Carbon* **68**, 175 (2014).
- [9] A. Wei, L. Xiong, L. Sun, Y. Liu, W. Li, W. Lai, X. Liu, L. Wang, W. Huang, X. Dong, *Mater Res Bull* **48**, 2855 (2013).
- [10] P. Jongnavakit, P. Amornpitoksuk, S. Suwanboon, N. Ndiege, *Appl Surf Sci* **258**, 8192 (2012).
- [11] L. Fu, Y. Zheng, Q. Ren, A. Wang, B. Deng, *Journal of Ovonic Research* **11**, 21 (2015).
- [12] H. Qin, W. Li, Y. Xia, T. He, *ACS applied materials & interfaces* **3**, 3152 (2011).
- [13] Z. Han, L. Ren, Z. Cui, C. Chen, H. Pan, J. Chen, *Appl Catal B-Environ* **126**, 298 (2012).
- [14] L. Fu, Y. Zheng, A. Wang, W. Cai, H. Lin, *Food Chemistry* **181**, 127 (2015).
- [15] S.-M. Lam, J.-C. Sin, A.Z. Abdullah, A.R. Mohamed, *Ceram Int* **39**, 2343 (2013).
- [16] K. Vignesh, A. Suganthi, M. Rajarajan, S.A. Sara, *Powder Technology* **224**, 331 (2012).
- [17] V. Eskizeybek, F. Sarı, H. Gülce, A. Gülce, A. Avcı, *Appl Catal B-Environ* **119–120**, 197 (2012).
- [18] L. Fu, Y. Zheng, Z. Wang, A. Wang, B. Deng, F. Peng, *Digest Journal of Nanomaterials and Biostructures* **10**, 117 (2015).
- [19] B. Xue, T. Sun, J.K. Wu, F. Mao, W. Yang, *Ultrason Sonochem* **22**, 1 (2015).
- [20] R. Adhikari, G. Gyawali, T. Sekino, S. Wahn Lee, *J Solid State Chem* **197**, 560 (2013).
- [21] Y. Zheng, A. Wang, H. Lin, L. Fu, W. Cai, *RSC Advances* **5**, 15425 (2015).
- [22] Y. Li, H. Zhang, Z. Guo, J. Han, X. Zhao, Q. Zhao, S.-J. Kim, *Langmuir* **24**, 8351 (2008).
- [23] L. Zhang, K.-H. Wong, Z. Chen, J.C. Yu, J. Zhao, C. Hu, C.-Y. Chan, P.-K. Wong, *Applied Catalysis A: General* **363**, 221 (2009).
- [24] L. Fu, A. Wang, Y. Zheng, W. Cai, Z. Fu, *Materials Letters* **142**, 119 (2015).
- [25] C. Hu, J. Guo, J. Qu, X. Hu, *Langmuir* **23**, 4982 (2007).
- [26] D. Wang, Y. Duan, Q. Luo, X. Li, J. An, L. Bao, L. Shi, *Journal of Materials Chemistry* **22**, 4847 (2012).
- [27] G.R. Li, T. Hu, G.L. Pan, T.Y. Yan, X.P. Gao, H.Y. Zhu, *J Phys Chem C* **112**, 11859 (2008).
- [28] X. Wang, Q. Zhang, Q. Wan, G. Dai, C. Zhou, B. Zou, *J Phys Chem C* **115**, 2769 (2011).
- [29] W. Liu, M. Ji, S. Chen, *J. Hazard. Mater.* **186**, 2001 (2011).
- [30] R. Dong, B. Tian, J. Zhang, T. Wang, Q. Tao, S. Bao, F. Yang, C. Zeng, *Catalysis Communications* **38**, 16 (2013).
- [31] C. Zeng, M. Guo, B. Tian, J. Zhang, *Chemical Physics Letters* **575**, 81 (2013).
- [32] H. Raj Pant, B. Pant, H. Joo Kim, A. Amarjargal, C. Hee Park, L.D. Tijing, E. Kyo Kim, C. Sang Kim, *Ceram Int* **39**, 5083 (2013).
- [33] J.H. Yang, J.H. Zheng, H.J. Zhai, L.L. Yang, *Cryst Res Technol* **44**, 87 (2009).
- [34] J.-M. Song, J. Zhang, J.-J. Ni, H.-L. Niu, C.-J. Mao, S.-Y. Zhang, Y.-H. Shen, *CrystEngComm* **16**, 2652 (2014).
- [35] C. Wu, L. Shen, Y.C. Zhang, Q. Huang, *Materials Letters* **66**, 83 (2012).
- [36] B. Krishnakumar, M. Swaminathan, *Spectrochimica acta. Part A, Molecular and biomolecular spectroscopy* **99**, 160 (2012).